

Chemical Compositions of Four Metal-poor Giants

Sunetra Giridhar

Indian Institute of Astrophysics; Bangalore, 560034 India

giridhar@iiap.ernet.in

David L. Lambert

Department of Astronomy; University of Texas; Austin, TX 78712-1083

[dll@astro.as.utexas.edu](mailto: dll@astro.as.utexas.edu)

Guillermo Gonzalez

Department of Astronomy; University of Washington; Seattle, WA 98195-1580

[gonzalez@astro.washington.edu](mailto: gonzalez@astro.washington.edu)

Gajendra Pandey

Department of Astronomy; University of Texas; Austin, TX 78712-1083

[pandey@astro.as.utexas.edu](mailto: pandey@astro.as.utexas.edu)

Received _____; accepted _____

ABSTRACT

We present the chemical compositions of four K giants CS 22877-1, CS 22166-16, CS22169-35 and BS 16085 - 0050 that have $[\text{Fe}/\text{H}]$ in the range -2.4 to -3.1 . Metal-poor stars with $[\text{Fe}/\text{H}] < -2.5$ are known to exhibit considerable star - to - star variations of many elements. This quartet confirms this conclusion. CS 22877-1 and CS 22166-16 are carbon-rich. There is significant spread for $[\alpha/\text{Fe}]$ within our sample where $[\alpha/\text{Fe}]$ is computed from the mean of the $[\text{Mg}/\text{Fe}]$, and $[\text{Ca}/\text{Fe}]$ ratios. BS 16085 - 0050 is remarkably α enriched with a mean $[\alpha/\text{Fe}]$ of $+0.7$ but CS 22169-35 is α -poor. The aluminium abundance also shows a significant variation over the sample. A parallel and unsuccessful search among high-velocity late-type stars for metal-poor stars is described.

Subject headings: stars:abundances – stars:chemically peculiar stars: late-type

1. Introduction

Chemical compositions of metal-poor stars have long been used to probe the history of the early Galaxy. As the number of very metal-poor stars having a well determined chemical composition has increased, it has become apparent that the metallicity, usually represented by the iron abundance [Fe/H], is not sufficient to predict the abundances of other elements; a real star-to-star scatter in abundance ratios [el/Fe] appears for many elements among stars more metal-poor than [Fe/H] of about -2. For stars in [Fe/H] range -2 to +0.3, the various [el/Fe] show almost no ‘cosmic’ scatter. In the light of the cosmic scatter shown by very metal-poor stars, it is important to analyse as large a sample of such stars as possible, in order to characterize fully the extent of the scatter. This paper represents a modest contribution to that end by presenting abundance analyses of four K giants with [Fe/H] \sim -2.4 to -3.1, and by describing an as yet unsuccessful search for late-type metal-poor stars in a list of stars of high tangential velocity.

2. Observations

A program of medium resolution spectroscopy was undertaken to identify metal-poor field stars from Lee’s (1984) list of stars with tangential velocities estimated to exceed 100 km s⁻¹. Lee compiled his lists from Lowell proper motions (Giclas, Burnham & Thomas 1971) and an estimate of the parallax (trigonometric or spectroscopic). We elected to concentrate on stars of spectral type K because major surveys of metal-poor stars have largely been restricted to earlier spectral types (cf. Carney et al. 1996). Stars of spectral type K provide opportunities to measure aspects of a star’s chemical composition not readily determinable from warmer stars. The stars observed with medium resolution are presented in Table 1. Estimates of the B or V magnitude, and spectral type are taken from SIMBAD. The radial velocity is measured from our spectra (see below). In addition to stars

from Lee's sample, we observed 3 stars from the HK survey undertaken by Beers, Preston, & Schectman (1985, 1992).

The Casségrain spectrograph at the 2.3m Vainu Bappu Telescope (VBT) at Kavalur (Prabhu, Anupama & Surendiranath 1998) was used for the spectroscopic survey. With the chosen grating of 1200 grooves mm^{-1} and a Tektronix 1024×1024 $24\mu\text{m}$ pixel CCD, the intermediate dispersion was 1.3\AA per pixel. The bright K subgiant (spectral type K1IV) star HR 4182 was observed as radial velocity standard and also as a near-solar metallicity representative.

These spectra enabled us to measure radial velocities (Table 1) to an accuracy of about $\pm 18 \text{ km s}^{-1}$ using cross-correlation task FXCORR contained in IRAF software. Our velocities are in fair agreement with the few previously published values located through SIMBAD (see footnotes to Table 1). From inspection of the spectra, it was obvious that five stars from Table 1 are extremely metal-poor: CS 22166-16, 22169-35, 22877-1, 22877-11, 22877-51. A metal deficiency for these stars was expected from the preliminary estimates of metallicity assigned by Beers et al. (1992). CS 22877-11 was the subject of a detailed abundance analysis reported by McWilliam et al. (1995) who gave the iron deficiency as $[\text{Fe}/\text{H}] = -2.9$. Strömgren photometry (Schuster et al. 1996) showed CS 22877-51 to be metal-poor ($[\text{Fe}/\text{H}] = -2.45$). Lee's star G 53-24 is given $[\text{Fe}/\text{H}] = 0.18$ by Ryan & Norris (1991).

The three very metal-poor stars from the Kavalur survey with BS 16085-0050 from Anthony-Twarog et al. (2000) were selected for an abundance analysis. They were observed with the Apache Point Observatory's 3.5 meter telescope and the vacuum-sealed echelle spectrograph. It uses a 31.6 line/mm echelle grating with a prism cross-disperser. The 2048x2048 SITe CCD has 24 micron pixels, resulting in a 2 pixel resolving power near 38,000. Due to the close spacing of the orders on the CCD, it is necessary to employ

nonstandard reduction methods. The most significant difference is the use of a hot star instead of lamp as a flat. As a measure of the quality of the spectra, we note that the S/N ratio (per pixel) in the continuum near 6700Å was about 70 (CS 22166-16), 60 (CS 22169-35), 75 (CS 22877-1), and 90 (BS 16085-0050).

3. Abundance Analysis

Inspection of the high-resolution spectra confirmed that the observed stars are very metal-poor. Hydrogen lines appeared normal with no indication of emission. Our abundance analysis was an entirely standard procedure, as described for example in our papers on the RV Tauri variables (cf. Giridhar, Lambert & Gonzalez 2000). A 1997 version of the spectrum synthesis code MOOG (Sneden 1973) was used with model atmospheres drawn from the grid computed by Kurucz (1993). Lines of Fe I and Fe II were used to derive the atmospheric parameters: effective temperature T_{eff} , surface gravity g , and the microturbulent velocity ξ_t . The requirement that the Fe abundance derived from Fe I lines be independent of excitation potential and equivalent width were used to derive T_{eff} and ξ_t , respectively. Then, the requirement that Fe I and Fe II lines return the same abundance was used to derive $\log g$. This use of ionization equilibrium was verified using the Ti I and Ti II lines. Given the number of lines and the accuracy of the equivalent widths (5-10%), we consider the uncertainties for these quite similar stars to be about ± 150 K in T_{eff} , ± 0.25 in $\log g$, and ± 0.2 km s⁻¹ in ξ_t . The iron abundance is determined to about ± 0.2 dex. Final results for the atmospheric parameters are given in Table 2. Inspection of the abundances derived for the individual stars (Table 3) show that ionization equilibrium of Ti and Fe is satisfied with very similar parameters; the abundance differences from Ti I and Ti II lines are equal to those from the Fe I and Fe II lines to within 0.15 dex for all stars.

Lines employed in this analysis are presented in the Table 4. The $\log gf$ -values are

taken from compilations provided by Luck (private communication) and McWilliam et al. (1995). We derived carbon abundance for CS 22877-1, CS 22166-16 and CS 22169-35 using CH band at 4310 to 4330Å . No CH line could be detected for BS 16085-0050 inspite of its low temperature. We used HFS parameters given in McWilliam et al. for Mn I lines at 4030, 4033 and 4034Å to synthesize this region for BS 16085-0050 to derive Mn abundance. The same could not be done for CS 22877-1, CS 22166-16 and CS 22169-35 as Mn I lines were contaminated by CH lines. Elemental abundances are given in Table 3 as [X/H] with the standard error derived from the line-to -line scatter, the number of adopted lines, and [X/Fe]. Uncertainties arising from likely errors in the atmospheric parameters can be assessed from Ryan, Norris & Beers (1996, Table 3 and entries for HD 122563). In almost all cases, our tabulated standard error is the dominant contributor to the total error; the standard error of the mean is formally smaller than that quoted by the square-root of the number of contributing lines.

4. Discussion

In the light of published results on the composition of extremely metal-poor stars, we commence our discussion by comparing and contrasting the four stars with previously analysed stars. This will be done using the ratio [X/Fe]. Our primary reference works are the surveys by McWilliam et al. (1995) and Ryan et al. (1996), and reviews by McWilliam (1997) and Norris (1999). Variation of [X/Fe] with [Fe/H] is well determined from [Fe/H] ~ 0 to [Fe/H] $\simeq -2$ with remarkably little true (cosmic) scatter as long as normal stars are considered (Lambert 1989; Wheeler, Sneden & Truran 1989). For [Fe/H] ≤ -2 , many relations change shape and slope and may develop a significant cosmic scatter. Our stars will be judged as normal if they fall within the range of [X/Fe] given in the reference works. It should be noted that the analytical tools (models, lines, etc.) used here are very similar

to those employed by McWilliam et al. and Ryan et al. and, both samples included not only dwarfs but giants similar to our stars. Therefore, systematic errors affecting our [X/Fe] should be similar to those of the reference works. Since our principal goal is to relate our stars to the previously analysed stars, we do not here concern ourselves with the systematic errors arising from defects in the analytical tools, e.g., the use of local thermodynamic equilibrium (LTE) when non-LTE effects may be significant.

4.1. CS 22877-1

This C-rich star at $[\text{Fe}/\text{H}] = -2.8$ has [X/Fe] firmly within the expected range except for Na (possibly underabundant), Al, and Ti (possibly slightly underabundant). The high C abundance is evident from the great strength of the CH bands: our estimate of $[\text{C}/\text{Fe}] = +1.8$ comes from a spectrum synthesis (Figure 1). Although this star is C-rich relative to most extremely metal-poor stars, its $[\text{C}/\text{Fe}]$ is matched by other stars (Norris, Ryan & Beers 1997). The Na abundance, $[\text{Na}/\text{Fe}] = -0.5$, is a little outside the range of -0.3 to +0.4 reported by McWilliam et al., also using the Na D lines. Figure 2 shows the Al I line at 3961\AA . The Al abundance, $[\text{Al}/\text{Fe}] = +0.2$, is within the large range of -1.0 to +0.5 found by McWilliam et al. from the 3961\AA Al I resonance line; the other resonance line at 3944\AA was shown by Arpigny & Magain (1983) to be blended with several CH lines, even in stars where CH was not the prominent feature of the spectrum that it is for CS 22877-1. Ryan et al.’s analyses of the resonance line, however, gave a rather well defined ‘plateau’ at $[\text{Al}/\text{Fe}] \simeq -0.8$ and relative to this value (and to points in their $[\text{Al}/\text{Mg}]$ vs $[\text{Fe}/\text{H}]$ plot), CS 22877-1 is Al-enriched but analysis of the 3961\AA line is sensitive to the adopted microturbulence. The origin of the difference between McWilliam et al.’s and Ryan et al.’s Al abundances is unclear, according to Ryan et al. Clearly, there is a need to probe this discrepancy more deeply because classification of Al abundances for the four stars as

‘normal’ or ‘abnormal’ depends on whether the appropriate set of reference abundances is that offered by McWilliam et al. or that by Ryan et al. We do not attempt to resolve the discrepancy. In Figure 3, we show the star’s location in $[X/Fe]$ versus $[Fe/H]$ plots for $X = Al, \alpha$, where α denotes Mg, and Ca. Abundances from McWilliam et al. and Ryan et al. are given as a reference. We chose not to include $[Si/Fe]$ as not many good Si I lines were accessible. The abundances of the three measured elements from Sr to Ba are each within the ranges defined by McWilliam et al. and Ryan et al.

4.2. CS 22166-16

CS 22166-16 at $[Fe/H] = -2.4$ is enriched in carbon relative to the typical value $[C/Fe] \simeq 0$ but to a more moderate and seemingly more common level than CS 22877-1. Other elements are at or close to their expected levels. Mg and Ca abundances are well determined and provide $[\alpha/Fe] = 0.6$. The Si abundance based on a single weak line is $[Si/Fe] = 0.2$. Chromium is underabundant at $[Cr/Fe] = -0.9$; McWilliam et al. and Ryan et al. find $[Cr/Fe] \simeq -0.2$ for $[Fe/H] = -2.4$ with a few outliers at lower $[Cr/Fe]$. Na has a normal abundance according to McWilliam et al.’s results. The abundances of Sr and Ba, the only measured heavy elements, fall within the cosmic scatter previously reported with $[Sr/Fe]$ at the lower boundary of previous results.

4.3. CS 22169-35

Relative to the expected composition of a $[Fe/H] = -2.9$ star, a striking aspect of CS 22169-35 is the low abundance of the α -elements Mg, Si, Ca, and Ti. Magnesium and calcium which are well represented give $[Mg/Fe] = 0.0$ and $[Ca/Fe] = 0.1$. Titanium from 9 Ti II lines gives $[Ti/Fe] = 0.0$ (Figure 3), a result consistent with that from the 2 Ti I lines.

The mean index $[\alpha/\text{Fe}]$ from Mg and Ca (Figure 3) is smaller than any index measured by McWilliam et al. and Ryan et al. McWilliam et al. found 3 stars with a $[\text{Mg}/\text{Fe}]$ well below the expected values, and one of these stars was also low in Ca, the only low Ca star in their sample. Carbon is slightly enriched: $[\text{C}/\text{Fe}] \simeq +0.4$ where $[\text{C}/\text{Fe}] \simeq 0.0$ is accepted as normal. Aluminium at $[\text{Al}/\text{Fe}] = -0.7$ is not exceptional and belongs to Ryan et al.’s plateau. Sodium from the Na D lines appears distinctly underabundant relative to McWilliam et al.’s sample at $[\text{Na}/\text{Fe}] = -0.7$.

A metal-poor star with low α -element abundances while unusual is not unprecedented. Our star is reminiscent of the pair HD 134439/134440 (King 1997; James 2000) at $[\text{Fe}/\text{H}] = -1.5$. These common proper motion stars have a higher Ba abundance ($[\text{Ba}/\text{Fe}] \simeq -0.2$ vs -1.1) but this may reflect the metallicity difference of 1.4 dex. At a metallicity closer to that of CS 22169-35, BD $+80^\circ 245$ (Carney et al. 1997; James 2000) with $[\text{Fe}/\text{H}] = -2.0$ has low abundances of the α -elements (Mg, Ca, and Ti at $[\alpha/\text{Fe}] \simeq -0.2$) and Ba ($[\text{Ba}/\text{Fe}] = -1.3$). James also found low Mg, and Ca (and Ba) but not Ti abundances in the star G 4-36 with $[\text{Fe}/\text{H}] = -2.0$. A group of α -poor stars with $[\text{Fe}/\text{H}] = -1.2$ to -0.6 was uncovered by Nissen & Schuster (1997) who delineated several abundance trends. Their correlation between $[\text{Na}/\text{Mg}]$ and $[\text{Mg}/\text{H}]$ does not extend to lower $[\text{Fe}/\text{H}]$ but our result, also the results by James (2000), suggests an approximately constant $[\text{Na}/\text{Mg}]$ at low $[\text{Fe}/\text{H}]$. On the other hand, the $[\text{Ni}/\text{Fe}]$ vs $[\text{Fe}/\text{H}]$ trend suggested by Nissen & Schuster is not satisfied by α -poor low $[\text{Fe}/\text{H}]$ stars.

4.4. BS 16085-0050

The outstanding aspect of this star’s composition, the most iron-deficient of the quartet at $[\text{Fe}/\text{H}] = -3.1$, is the high abundance of the α -elements. With $[\alpha/\text{Fe}] = 0.9, 1.2$, and 0.6 for Mg, Si, and Ca, respectively, it is unmatched by any of Ryan et al.’s stars. McWilliam

et al. found one star with similarly high $[\alpha/\text{Fe}]$ values: CS 22949-037 with $[\alpha/\text{Fe}] = +1.2$, 0.9, and 0.9 for Mg, Si, and Ca, respectively, and $[\text{Fe}/\text{H}] = -4.0$. Titanium sometimes grouped with the α -elements is a little below its expected abundance at $[\text{Ti}/\text{Fe}] = 0.2$. In CS 22949-037, Ti is only marginally above its expected value.

BS 16085-0050's high abundance of α -elements is a robust result. A high $[\alpha/\text{Fe}]$ is clearly indicated for Mg and Ca. Magnesium is represented by 7 Mg I lines including 2 strong lines and 5 weaker lines. Seven medium-strong Ca I lines give consistent results. If the atmospheric parameters are varied by their estimated uncertainties $[\text{Mg}/\text{Fe}]$ and $[\text{Ca}/\text{Fe}]$ do not vary by more than about ± 0.05 . No plausible change can reduce the best estimates $[\text{Mg}/\text{Fe}] = 0.9$ and $[\text{Ca}/\text{Fe}] = 0.6$ to the lower more typical values. Silicon is represented by just 2 lines. Variation of the atmospheric parameters has a larger effect on the $[\text{Si}/\text{Fe}]$ ratio because in part the Si I lines are sensitive to the adopted microturbulence but the effect is much smaller than the difference between the estimated $[\text{Si}/\text{Fe}] = 1.2$ and the lower value from the published surveys. Titanium for which adequate samples of Ti I and Ti II lines provide consistent results clearly gives a lower ratio of $[\text{Ti}/\text{Fe}] = 0.2$ with very little sensitivity to the atmospheric parameters. In summary, Mg and Ca and most likely Si but not Ti are unusually enriched in this star. Magnesium and calcium are well represented in all stars and, therefore, the star-to-star differences in $[\alpha/\text{Fe}]$ are considered real.

Aluminum is approximately normal judged by McWilliam et al.'s range in $[\text{Al}/\text{Fe}]$, and by Ryan et al.'s $[\text{Al}/\text{Mg}]$ but not their $[\text{Al}/\text{Fe}]$ range where BS 16085-0050 appears overabundant in Al. Heavy elements Sr, Y, and Ba fall just within the previously reported spreads for stars with $[\text{Fe}/\text{H}] \sim -3$. Their $[\text{X}/\text{Fe}]$ values are at the lower boundaries of previous results.

5. Concluding Remarks

A somewhat surprising outcome of our initial survey of Lee's high velocity stars is the absence of metal-poor stars. Most stars appear to have an abundance near solar. Given that the selection criterion was a tangential velocity in excess of 100 km s^{-1} , we expected to find a rather metal-poor sample. This apparent puzzle will be considered when our survey is more complete.

Our modest addition to the number of very metal-poor stars subjected to an abundance analysis reveals several interesting facets about these stars. Two of the stars are evidently very rich in carbon. This is not an uncommon feature of very metal-poor stars (Rossi, Beers & Sneden 1999). At solar metallicities, carbon-enrichment of a stellar atmosphere is widely associated with enrichment of *s*-process elements and attributed to contamination of the star by mass-transfer from an AGB star. This attribution is far less appropriate for very metal-poor stars. Several C-enriched stars have been shown not to be binaries (Norris et al. 1997) and in addition the C-enrichment is not always coupled with *s*-process enrichment. In short, mass transfer is a plausible explanation in only some cases and in others the C-enrichment was likely present in the star's natal cloud. In the case of CS 22877-1 and probably also CS 22877-16, the carbon enrichment is not related to the *s*-process but heavy elements point to an *r*-process connection. Whether these stars are binaries or not is presently unknown.

Very metal-poor stars are apparently not a monolithic block with respect to the ratio of α -elements to iron. BS 16085-0050 is α -enriched at a level rarely seen previously but this enrichment is not unprecedented: CS 22949-37 is similar (McWilliam et al. 1995). At the other extreme, CS 22169-35 joins a small group of α -poor very metal-poor stars. Star-to-star spread in elemental abundance ratios with respect to iron are seen in some other elements, particularly the heavy elements where a considerable dispersion has been

noted previously.

The large spread in abundances particularly for α elements found for stars with $[\text{Fe}/\text{H}] < -2.5$ indicate that before this metallicity level was attained, the early Galaxy experienced very unusual chemical enrichment. Refinement of supernovae models are perhaps required to explain uneven yield of α elements. Galactic chemical enrichment models including the effect of incomplete mixing might help in explaining the observed abundance peculiarities. Perhaps, the principal lesson to be drawn from our small sample is that not everything has yet been gleaned from abundance analyses of very metal-poor stars. The mine is not yet exhausted of valuable ores.

At the University of Texas, this research was supported in part by the National Science Foundation (grant AST-9618414) and the Robert A. Welch Foundation.

6. references

Anthony-Twarog, B.J., Sarajedini, A., Twarog, B.A., & Beers, T.C. 2000, AJ, 119, 2882

Arpigny, C., & Magain, P. 1983, A&A, 127, L7

Beers, T.C., Preston, G.W., & Schectman, S.A. 1985, AJ, 90, 2089

Beers, T.C., Preston, G.W., & Schectman, S.A. 1992, AJ, 103, 1987

Carney, B.W., Laird, J.B., Latham, D.W., & Aquilar, L.A. 1996, AJ, 112, 668

Carney, B.W., Wright, J.S., Sneden, C., Laird, J.B., Aguilar, L.A., & Latham, D.W. 1997, AJ, 114, 363

Giclas, H.L., Burnham, R. Jr., & Thomas, N.G., 1971, Lowell Proper Motion Survey -

Northern Hemisphere, Lowell Observatory.

Giridhar, S., Lambert, D.L., & Gonzalez, G. 2000, ApJ, 531, 521

James, C.R. 2000, PhD Thesis, Univ. of Texas at Austin

King, J.R. 1997, AJ, 113, 2302

Kurucz, R.L., 1993, ATLAS9 Stellar Atmosphere Programs and 2 km s^{-1} grid, CDROM 13, Smithsonian Astrophysical Observatory

Lambert, D.L. 1989, in *Cosmic Abundances of Matter*, ed. C.J. Waddington, AIP Conf. Proc. 183, 168

Lèbre, A., de Laverny, P., de Medeiros, J.R., Charbonnel, C., da Silva, L. 1999, A&A, 345, 936

Lee, S.-G. 1984, AJ, 89, 720.;

McWilliam, A. 1997, ARAA, 35, 503

McWilliam, A., Preston, G.W., Sneden, C., & Searle, L. 1995, AJ, 109, 2757

Nissen, P.E., & Schuster, W.J. 1997, A&A, 326, 751

Norris, J.E. 1999, in *The Third Stromlo Symposium: The Galactic Halo*, ed. B.K. Gibson, T.S. Axelrod, & M.E. Putman, ASP Conf. Ser., 165, 213

Norris, J.E., Ryan, S.G., & Beers, T.C. 1997, ApJ, 488, 350

Prabhu, T.P., Anupama, G.C., & Surendiranath, R. 1998, BASI, 26, 383

Rossi, S., Beers, T.C., & Sneden, C. 1999, in *The Third Stromlo Symposium: The Galactic Halo*, ed. B.K. Gibson, T.S. Axelrod, & M.E. Putman, ASP Conf. Ser., 165, 264

Ryan, S.G., & Norris, J.E. 1991, AJ, 101, 1835

Ryan, S.G., Norris, J.E., & Beers, T.C. 1996, ApJ, 471, 254

Schuster, W.J., Nissen, P.E., Parrao, L., Beers, T.C., & Overgaard, L.P. 1996, A&AS, 117, 317

Sneden C. 1973, PhD Thesis, Univ. of Texas

Wheeler, J.C., Sneden, C., & Truran, J.W. 1989, ARAA, 27, 279

7. Figure Captions

Fig. 1.— Observed and synthetic spectra of CS 22877-1 at high resolution showing CH lines. The synthetic spectrum is computed for $[C/Fe] = +1.8$.

Fig. 2.— Observed spectra of CS 22877-1 and BS 16085 - 0050 showing Al I line at 3961\AA .

Fig. 3.— $[X/Fe]$ vs $[Fe/H]$ for $X = \text{Al}$, α and Mn where $[\alpha/Fe]$ is the mean of $[\text{Mg}/\text{Fe}]$ and $[\text{Ca}/\text{Fe}]$. Abundances from McWilliam et al. and Ryan et al. are given as reference.

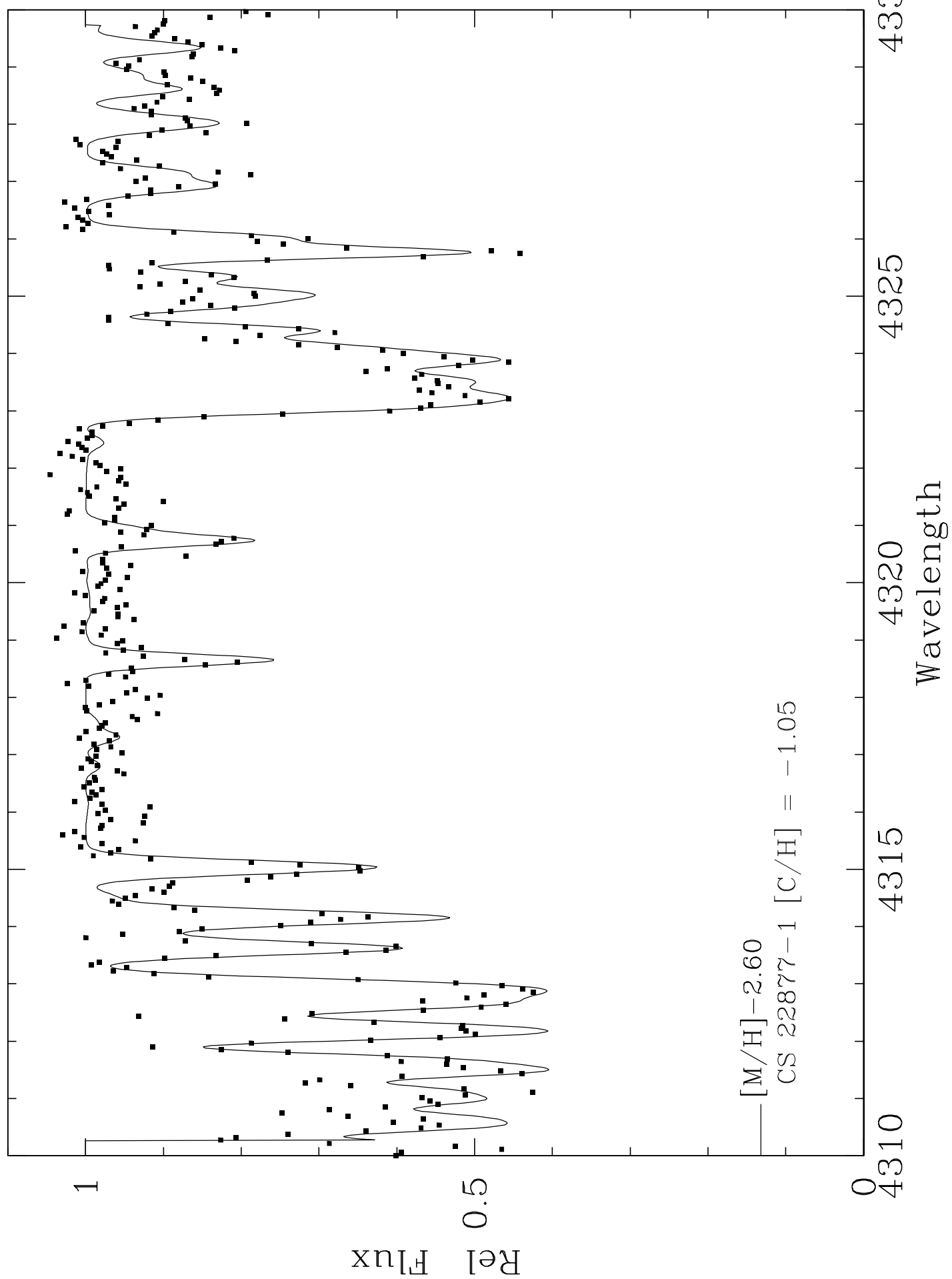


TABLE 1
BASIC DATA FOR SAMPLE STARS

Star	V or B ^a	Sp.Type	Rad. Vel. ^{b,c} km s ⁻¹
CS 22166-16	12.7	...	-212
CS 22169-35	12.9	...	+12
G 6-44	10.6	K0	-16
G 8-30	11.7	K3	-62
G 191-38	13.3*	K5	-35
G 99-24	10.8	K4	+62
G 106-25	10.9	K4	-58
G 104-22	12.4*	K2	-83
G 111-22	9.6	K2	+30
G 111-28	10.4	K0	-50
G 111-40	12.6*	K3	+30
G 115-1	12.5	K0	+60
G 252-26	10.6	K3	+31
G 41-29	15.4*	K1	-34
G 115-66	10.5	K0	+36
G 53-24	11.7	K2	+72
G 253-37	10.7	K4	-17
G 122-30	11.2	K	-71
BS 16085-0050	12.1	...	-72
CS 22877-1	+165
CS 22877-11	13.9
CS 22877-51	14.2*	...	+285

^a The entry in the second column with * shows B magnitude

^b The radial velocities measured by Beers et al. 1992 for CS stars are -215, +2, +169, +215 and 276 km s⁻¹ in the order of their appearance in the table1.

^c The radial velocity value of -69 km s⁻¹ was reported for G106-25 by Ryan and Norris.

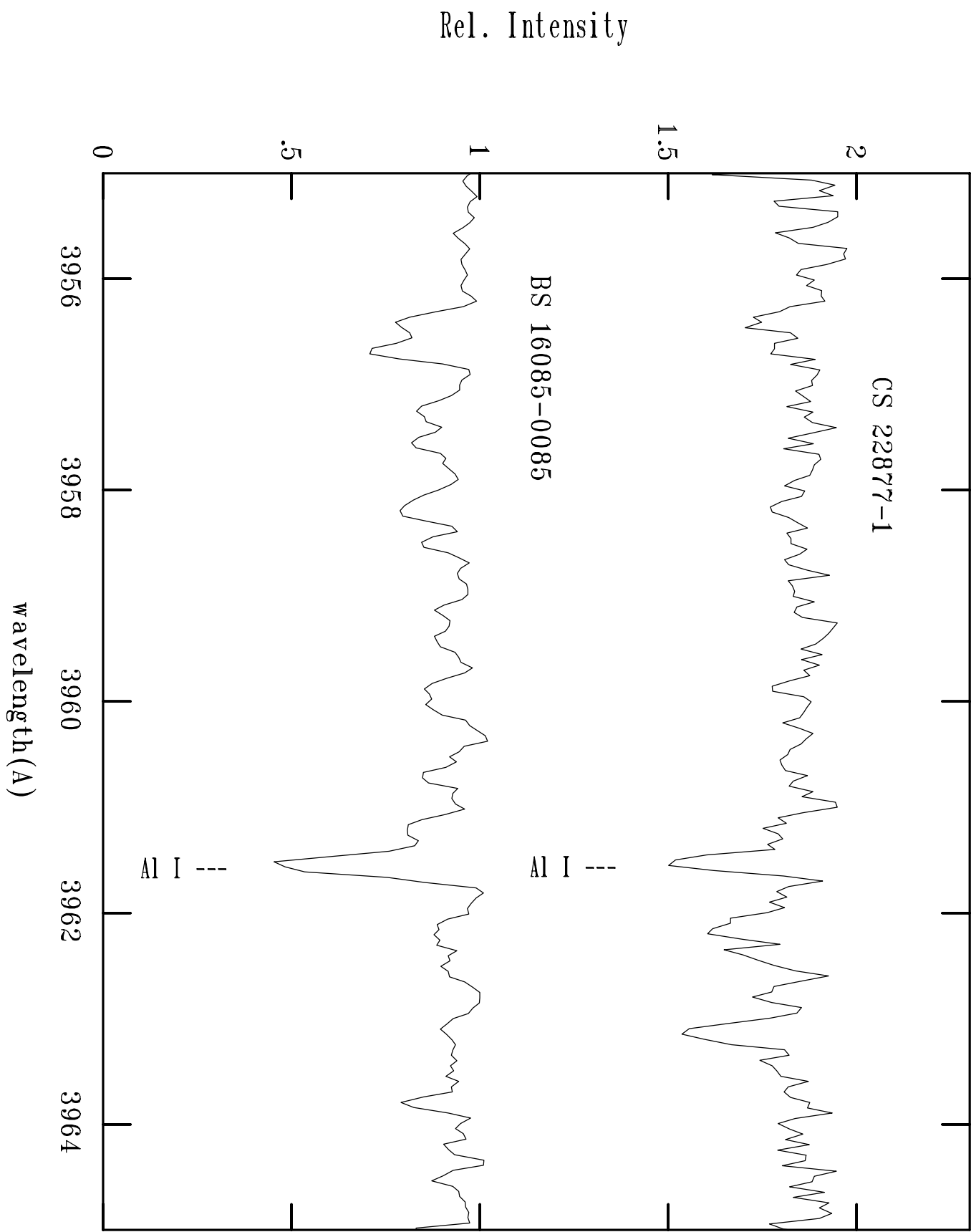


TABLE 2
STELLAR PARAMETERS DERIVED FROM THE FE-LINE ANALYSES

Star UT Date	Model ^a T_{eff} , $\log g$, [Fe/H]	ξ_t (km s $^{-1}$)	Fe I ^b		Fe II	
			$\log \epsilon$	n	$\log \epsilon$	n
CS 22877-1 2000 Dec 31	5000, 1.5, -2.8	2.3	4.69 ± 0.18	55	4.63 ± 0.20	10
CS 22166-16 1999 Dec 31	5250, 2.0, -2.4	2.2	5.11 ± 0.19	33	5.06 ± 0.22	8
CS 22169-35 2000 Jan 5	4500, 1.0, -2.8	2.6	4.65 ± 0.17	34	4.66 ± 0.11	5
BS 16085-0050 2000 Mar 24	4750, 1.0, -3.1	2.3	4.36 ± 0.17	30	4.45 ± 0.15	9

^a T_{eff} in K, $\log g$ in cgs, [Fe/H] in dex.

^b $\log \epsilon$ is the mean abundance relative to H (with $\log N_{\text{H}} = 12.00$). The solar value of $\log \epsilon$ (Fe) is 7.51. The standard deviations of the means, as calculated from the line-to-line scatter, are given. n is the number of considered lines.

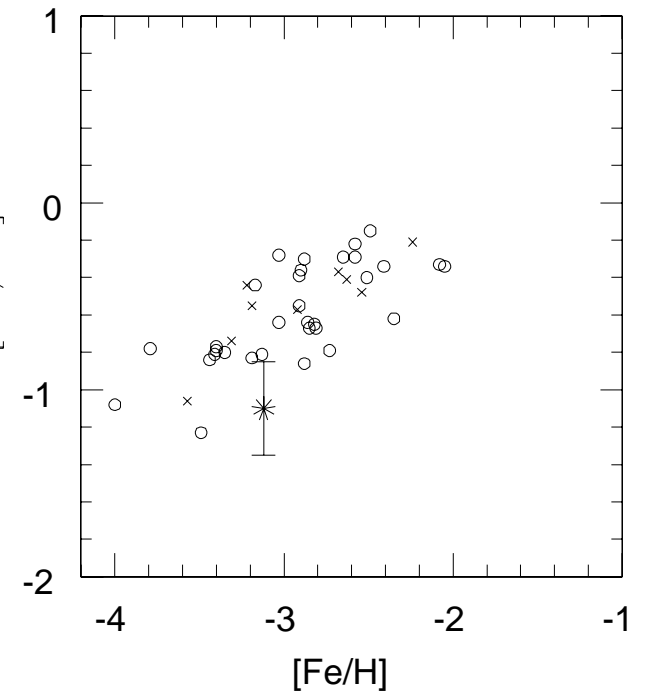
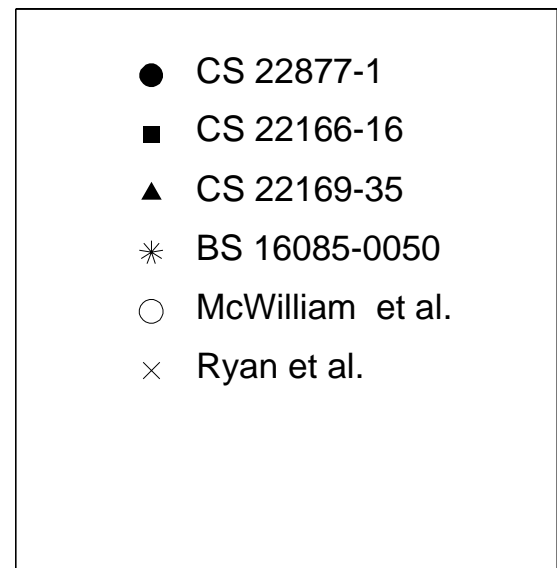
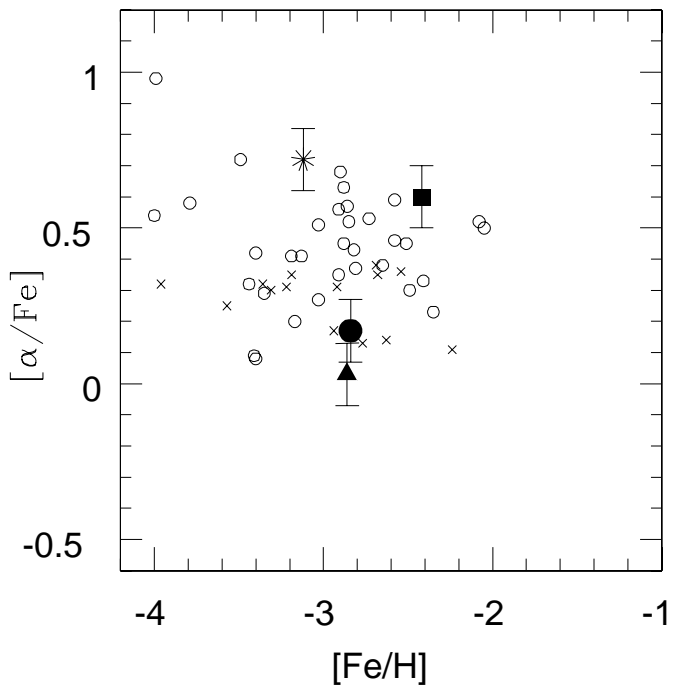
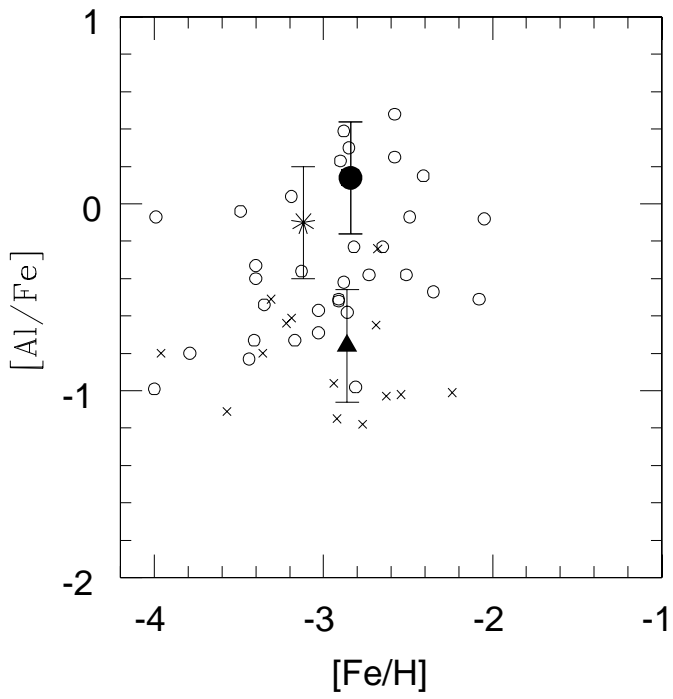


TABLE 3
ELEMENTAL ABUNDANCES FOR CS 22877-1, CS 22166-16, CS 22169-35 & BS 16085-00

Species	$\log \epsilon_{\odot}$	CS 22877-1			CS 22166-16			CS 22169-35		
		[X/H]	no. of lines	[X/Fe]	[X/H]	no. of lines	[X/Fe]	[X/H]	no. of lines	[X/Fe]
C I	8.55	-1.05	syn	+1.80	-1.40	syn	+1.02	-2.45	syn	+0.40
Na I	6.33	-3.31 \pm 0.03	2	-0.47	-2.05 \pm 0.20	2	+0.37	-3.56 \pm 0.10	2	-0.70
Mg I	7.58	-2.70 \pm 0.15	5	+0.14	-1.74 \pm 0.22	4	+0.68	-2.86 \pm 0.12	4	+0.01
Al I	6.47	-2.70 \pm 0.07	2	+0.14	-3.61 \pm 0.39	2	-0.76
Si I	7.55	-2.76	1	+0.08	-2.20	1	+0.22	-3.11 \pm 0.60	2	-0.26
Ca I	6.35	-2.53 \pm 0.06	6	+0.31	-1.92 \pm 0.15	7	+0.50	-2.77 \pm 0.11	7	+0.08
Sc II	3.13	-2.71	1	-0.13	-1.94 \pm 0.09	3	+0.48	-2.59 \pm 0.10	3	-0.26
Ti I	4.98	-2.68 \pm 0.03	3	+0.16	-2.24 \pm 0.25	2	+0.18	-2.93 \pm 0.10	2	-0.08
Ti II	4.98	-2.88 \pm 0.12	7	-0.04	-2.27 \pm 0.21	6	+0.15	-2.83 \pm 0.18	9	-0.02
Cr I	5.67	-3.02 \pm 0.07	2	-0.18	-3.27 \pm 0.30	4	-0.85	-3.24 \pm 0.21	4	-0.39
Mn I	5.39
Fe I	7.51	-2.82 \pm 0.18	55	...	-2.40 \pm 0.19	33	...	-2.86 \pm 0.17	34	...
Fe II	7.51	-2.88 \pm 0.20	10	...	-2.45 \pm 0.22	8	...	-2.85 \pm 0.11	4	...
Co I	4.91	-2.49	1	+0.35
Ni I	6.25	-2.91 \pm 0.08	3	-0.07	-2.25 \pm 0.18	2	+0.17	-2.71 \pm 0.21	4	+0.14
Sr II	2.90	-3.23	1	-0.38	-3.43 \pm 0.3	2	-1.01
Y II	2.24	-3.11	1	-0.27
Ba II	2.13	-3.36 \pm 0.20	4	-0.52	-2.80 \pm 0.20	3	-0.37	-3.92 \pm 0.31	4	-1.07
Ce II	1.55	-2.11	1	+0.74

TABLE 4: EQUIVALENT WIDTHS FOR THE LINES USED

Ion	Wavelength (Å)	low E.P. (ev)	log gf	CS 22877-1 W_λ (mÅ)	CS 22166-16 W_λ (mÅ)	CS 22169-35 W_λ (mÅ)	BS 16085-50 W_λ (mÅ)
Na I	5889.94	0.00	0.11	112	181	128	137
Na I	5895.94	0.00	-0.19	89	141	113	125
Mg I	4057.52	4.34	-1.00	26
Mg I	4167.28	4.34	-0.94	46
Mg I	4571.10	0.00	-5.74	22	42	...	43
Mg I	4703.00	4.34	-0.38	38	...	47	68
Mg I	5172.70	2.72	-0.38	142	212	164	202
Mg I	5183.62	2.72	-0.16	155	251	183	205
Mg I	5528.42	4.34	-0.34	36	79	46	51
Al I	3944.02	0.00	-0.63	128	...	90	113
Al I	3961.53	0.00	-0.32	147	...	130	117
Si I	3905.53	1.91	-0.98	...	122	112	178
Si I	4102.94	1.91	-2.72	30	50	60	99
Ca I	4302.60	1.90	-0.15	59
Ca I	4425.44	1.88	-0.36	31	29
Ca I	5588.76	2.52	0.36	34	60	36	34
Ca I	5594.47	2.52	0.09	28
Ca I	5598.49	2.52	-0.09	17	35
Ca I	6102.72	1.88	-0.80	21
Ca I	6122.23	1.89	-0.32	41	65	41	52
Ca I	6162.18	1.90	-0.09	48	70	64	56
Ca I	6439.08	2.52	0.39	...	83	44	49
Ca I	6493.79	2.52	-0.11	...	38	27	...
Ca I	6499.65	2.52	-0.82	...	17
Sc II	4246.84	0.31	0.02	108	122	...	123
Sc II	4320.75	0.61	-0.47	81
Sc II	5031.02	1.36	-0.57	39
Sc II	5239.82	1.45	-0.94	...	22	19	...
Sc II	5526.82	1.77	-0.22	28	34
Sc II	5657.88	1.51	-0.82	...	20	24	...
Ti I	4533.24	0.84	0.48	25	23
Ti I	4533.97	0.85	0.53	...	30
Ti I	4534.78	0.84	0.34	30	18
Ti I	4981.74	0.85	0.52	33	43
Ti I	4991.07	0.84	0.41	25	26
Ti I	4999.51	0.83	0.31	32	...
Ti I	5014.24	0.00	-1.16	...	15
Ti II	4163.66	2.59	-0.39	30
Ti II	4290.23	1.18	-1.12	83	89
Ti II	4337.93	1.08	-1.13	74

TABLE 4: EQUIVALENT WIDTHS FOR THE LINES USED—Continued

Ion	Wavelength (Å)	low E.P. (ev)	log gf	CS 22877-1 W_λ (mÅ)	CS 22166-16 W_λ (mÅ)	CS 22169-35 W_λ (mÅ)	BS 16085-50 W_λ (mÅ)
Ti II	4394.06	1.22	-1.77	34
Ti II	4395.04	1.56	-0.51	103	...
Ti II	4395.85	1.24	-1.96	27
Ti II	4417.72	1.16	-1.43	72	...
Ti II	4443.81	1.08	-0.70	...	98	...	112
Ti II	4464.46	1.16	-1.79	29	...	57	24
Ti II	4468.50	1.13	-0.59	95	...	130	95
Ti II	4501.28	1.12	-0.76	91	97	110	...
Ti II	4529.49	1.57	-1.72	15
Ti II	4533.97	1.24	-0.78	79	101	110	97
Ti II	4563.77	1.22	-0.78	75	112	86	89
Ti II	4571.96	1.57	-0.53	72	...	106	75
Ti II	4589.95	1.24	-1.64	39	57
Ti II	5154.08	1.57	-1.77	...	30
Ti II	5336.79	1.58	-1.65	...	34
Cr I	4254.35	0.00	-0.11	103	69	...	81
Cr I	4274.81	0.00	-0.23	...	72	...	92
Cr I	4289.73	0.00	-0.36	93	45	...	93
Cr I	4558.60	4.07	-0.66	11
Cr I	5206.04	0.94	0.02	61	...
Cr I	5208.43	0.94	0.16	69	69	101	...
Cr I	5345.81	1.00	-0.98	37	...
Cr I	5409.80	1.03	-0.72	22	...	38	18
Fe I	3808.73	2.56	-1.16	19
Fe I	3846.42	3.57	-0.43	26
Fe I	3878.03	0.96	-0.91	115
Fe I	3949.96	2.18	-1.16	53	45
Fe I	4005.25	1.56	-0.61	115	94
Fe I	4175.64	2.84	-0.67	21
Fe I	4199.11	3.05	0.25	83
Fe I	4222.22	2.22	-0.97	37
Fe I	4250.14	2.47	-0.40	68
Fe I	4260.49	2.40	-0.02	98	102	87	...
Fe I	4271.77	1.49	-0.16	125
Fe I	4383.56	1.48	0.20	138
Fe I	4388.41	3.60	-0.59	...	20
Fe I	4430.62	2.22	-1.65	33	17
Fe I	4442.35	2.20	-1.25	54	47
Fe I	4447.73	2.22	-1.34	54
Fe I	4459.14	2.18	-1.27	33
Fe I	4489.75	0.12	-3.97	75	...
Fe I	4494.57	2.20	-1.14	55	...	92	50
Fe I	4531.16	1.48	-2.17	53	53	...	43
Fe I	4678.85	3.60	-0.66	...	31
Fe I	4871.33	2.86	-0.27	58

TABLE 4: EQUIVALENT WIDTHS FOR THE LINES USED—Continued

Ion	Wavelength (Å)	low E.P. (ev)	$\log gf$	CS 22877-1 W_λ (mÅ)	CS 22166-16 W_λ (mÅ)	CS 22169-35 W_λ (mÅ)	BS 16085-50 W_λ (mÅ)
Fe I	4872.14	2.88	-0.50	44	...	64	33
Fe I	4918.99	2.86	-0.34	47	...	84	47
Fe I	4920.51	2.83	0.07	68	68
Fe I	5014.95	3.94	-0.27	...	19
Fe I	5041.08	0.96	-2.89	49	35
Fe I	5049.82	2.28	-1.35	39	...	58	38
Fe I	5051.64	0.91	-2.78	55	65	93	46
Fe I	5079.23	2.20	-2.06	28
Fe I	5083.35	0.96	-2.91	41	39
Fe I	5123.72	1.01	-3.07	44	44	89	...
Fe I	5133.70	4.18	0.20	25
Fe I	5150.85	0.99	-3.00	31
Fe I	5151.92	1.01	-3.32	27	41	51	...
Fe I	5162.28	4.18	0.08	25	...	28	...
Fe I	5171.61	1.49	-1.76	...	71
Fe I	5194.95	1.56	-2.06	44	62	80	...
Fe I	5198.72	2.22	-2.14	...	28
Fe I	5202.35	2.18	-1.84	30
Fe I	5216.28	1.61	-2.12	43	50	94	...
Fe I	5232.95	2.94	-0.08	51	71	87	...
Fe I	5250.65	2.20	-2.05	33	...
Fe I	5281.80	3.04	-0.83	33
Fe I	5324.19	3.21	-0.10	48
Fe I	5328.05	0.91	-1.63	115	115
Fe I	5332.91	1.56	-2.94	30	...
Fe I	5339.94	3.26	-0.68	21
Fe I	5341.03	1.61	-1.95	55
Fe I	5371.50	0.96	-1.65	114
Fe I	5383.38	4.31	0.65	15	45
Fe I	5393.17	3.24	-0.72	15	47	37	...
Fe I	5405.79	0.99	-1.85	96	91	136	96
Fe I	5415.21	4.39	0.50	24
Fe I	5424.08	4.32	0.58	32
Fe I	5434.53	1.01	-2.12	91	91	127	103
Fe I	5446.92	0.99	-1.91	93	113	143	93
Fe I	5497.53	1.01	-2.84	49	65	...	46
Fe I	5501.48	0.96	-2.95	94	...
Fe I	5506.79	0.99	-2.80	50	50	102	53
Fe I	5586.77	3.37	-0.12	31	53	...	38
Fe I	5615.66	3.33	0.05	48	57	...	39
Fe I	6136.62	2.45	-1.40	27	40	67	...
Fe I	6137.70	2.59	-1.40	24	34	50	31
Fe I	6191.57	2.43	-1.42	32	46	57	...
Fe I	6213.44	2.22	-2.48	22	...
Fe I	6230.76	2.56	-1.28	...	28
Fe I	6252.57	2.40	-1.72	24	34
Fe I	6393.61	2.43	-1.43	33	33	41	43

TABLE 4: EQUIVALENT WIDTHS FOR THE LINES USED—Continued

Ion	Wavelength (Å)	low E.P. (ev)	$\log gf$	CS 22877-1 W_λ (mÅ)	CS 22166-16 W_λ (mÅ)	CS 22169-35 W_λ (mÅ)	BS 16085-50 W_λ (mÅ)
Fe I	6400.01	3.60	-0.07	21	30
Fe I	6411.66	3.65	-0.66	13	13
Fe I	6421.36	2.28	-2.01	...	28	46	...
Fe I	6430.86	2.18	-2.01	...	33	45	...
Fe I	6678.00	2.69	-1.42	...	38	47	13
Fe II	4173.47	2.58	-2.18	72	62
Fe II	4178.87	2.58	-2.48	40
Fe II	4233.17	2.58	-1.91	...	73	...	60
Fe II	4385.38	2.78	-2.70	29
Fe II	4416.83	2.78	-2.60	37
Fe II	4491.40	2.85	-2.59	32
Fe II	4508.29	2.85	-2.31	33	32
Fe II	4515.34	2.84	-2.48	41	37
Fe II	4555.89	2.83	-2.29	54	...
Fe II	4583.84	2.81	-2.02	54	84
Fe II	4731.45	2.89	-2.92	...	22
Fe II	4923.93	2.89	-1.43	79	81	...	82
Fe II	5018.45	2.89	-1.22	98	97	111	101
Fe II	5169.03	2.89	-0.87	...	141
Fe II	5197.58	3.23	-2.25	28	30	33	...
Fe II	5234.63	3.22	-2.24	18	...	35	...
Fe II	5276.00	3.20	-1.91	24
Fe II	6456.39	3.90	-2.20	...	20
Co I	3995.32	0.92	-0.22	67	72
Co I	4020.91	0.43	-2.07	18
Co I	4121.33	0.92	-0.32	64
Ni I	3807.15	0.42	-1.18	93
Ni I	3858.30	0.42	-0.97	96
Ni I	5017.58	3.54	-0.08	...	16
Ni I	5476.92	1.83	-0.89	53	57	73	68
Ni I	6108.13	1.68	-2.45	23	...
Ni I	6643.64	1.68	-2.30	20	...
Ni I	7122.21	3.54	0.04	25	...
Sr II	4077.75	0.00	0.15	...	97	...	59
Sr II	4215.54	0.00	-0.16	119	105	...	47
Y II	3950.36	0.10	-0.51	26
Ba II	4554.04	0.00	0.12	95	100	84	34
Ba II	4934.10	0.00	-0.15	82	90	...	20
Ba II	5853.69	0.60	-1.00	18	...
Ba II	6141.73	0.70	-0.07	30	43	18	10
Ba II	6496.90	0.60	-0.37	18	34	23	9
Ce II	4562.37	0.48	0.32	40	...